Available online at BCREC website: https://bcrec.id

Bulletin of Chemical Reaction Engineering & Catalysis, 17 (1) 2022, 103-112

Research Article

Synthesis of Porous N-doped TiO_2 by Using Peroxo Sol-Gel Method for Photocatalytic Reduction of Cd(II)

Diana Vanda Wellia*, Dina Nofebriani, Nurul Pratiwi, S. Safni

Department of Chemistry, Faculty of Mathematics and Natural Science, Universitas Andalas, 25163, Indonesia.

Received: 23rd September 2021; Revised: 26th November 2021; Accepted: 27th November 2021
Available online: 14th December 2021; Published regularly: March 2022

Abstract

Porous N-doped TiO_2 photocatalyst was successfully synthesized by an environmentally friendly peroxo sol-gel method using polyethylene glycol (PEG) as a templating agent. Here, the effect of PEG addition to the aqueous peroxotitanium solutions on the structure, pore properties and photocatalytic activity of the obtained photocatalysts was systematically studied. The prepared photocatalysts were characterized by X-ray diffraction (XRD), UV-Vis diffuse reflectance spectroscopy (DRS), and Brunauer-Emmett-Teller (BET). It was found that the doping of nitrogen narrows the band gap of TiO_2 leading to enhance its visible-light response. The BET analysis shows that the prepared photocatalysts have a typical mesoporous structure with pore sizes of 3–6 nm. The photocatalytic activity of the prepared photocatalysts was evaluated by photocatalytic reduction of Cd(II) in an aqueous solution under visible light irradiation. The results show that porous N-doped TiO_2 with the optimal PEG addition had the highest Cd(II) reduction of 85.1% after 2.5 h irradiation in neutral aqueous solution. This significant improvement in photocatalytic activity of the prepared photocatalysts was mainly attributed to the synergistic combination of N doping and porous structure, which could actively increase the catalytic active site of this photocatalysts.

Keywords: TiO_2; nitrogen doping; mesoporous; photocatalyst; Cd(II) reduction

How to Cite: D.V. Wellia, D. Nofebriani, N. Pratiwi, S. Safni (2022). Synthesis of Porous N-doped TiO_2 by Using Peroxo Sol-Gel Method for Photocatalytic Reduction of Cd(II). *Bulletin of Chemical Reaction Engineering & Catalysis*, 17(1), 103-112 (doi: 10.9767/bcrec.17.1.12347.103-112)

Permalink/DOI: https://doi.org/10.9767/bcrec.17.1.12347.103-112

1. Introduction

The cadmium ion (Cd(II)) is one of the most toxic heavy metal that poses a serious threat to animal, environment and human health [1]. This ion could be easily found in the wastewater of many industries, including fossil fuel, battery manufacturing, metal plating, fertilizer, cement nonferrous, electroosmotic, electrolysis, photography, mining, and nuclear industries, [2–4]. Through this contaminant wastewater, Cd(II) would be introduced into the aquatic ecosystem and furthermore absorbed and accumulated in living tissues of organisms [5,6]. The accumulated Cd(II) in the human body can cause several health issues such as reproductive damage, liver cirrhosis, atrophy in the bone, and eventually death [7–9]. The most severe past tragedy due to Cd(II) contamination in the aquatic system was the "Itai-itai' disease outbreak, which occurred in Jinzu river, Toyama Prefecture, Japan starting from the 1910s [8,10,11]. Conventional treatment methods such as ion exchange [12], electrochemical method [13], precipitation [14], membrane technologies [15], and adsorption [16] have been used to remove Cd(II) from aqueous solution [17]. Mostly, all of these methods are only captured and transformed the Cd(II) ion from one phase into another phase, which means that Cd(II) is not

* Corresponding Author.
Email: nandadiana@sci.unand.ac.id (D.V. Wellia)

completely removed and still exist in its toxic form [18]. Therefore, it is important to develop an efficient method where Cd(II) can be reduced into its non-toxic oxidation state [19].

The heterogeneous photocatalytic process, which occur on the surface of semiconductor photocatalysts, has been considered to be an alternative-promising way in addressing the above limitation [20–22]. This process can activate and undertake both oxidation and reduction reactions under irradiation of light energy [23]. By conducting this method for the metal ion treatment, especially in the removal of Cd(II), this heavy metals would be directly reduced from its toxic ionic phase (Cd(II)) into non-toxic metallic phase (Cd(0)) [24-26]. It is believed that the photocatalytic method for the removal of heavy metals pollutants is more green, clean and economical than the conventional methods [27,28].

Among the various semiconductor photocatalyst, titanium dioxide semiconductor (TiO_2) has been widely used and extensively studied for the environmental treatment and water purification due to its non-toxic, inertness, chemically stable, low-cost, and highly photoactive properties [29–33]. TiO_2 can exist in three crystallographic forms: anatase, rutile and brookite. Among these crystal form, anatase was reported to be the most favorable due to lighter effective mass, smaller particle size and longer lifetime of photoexcited electrons and holes, leading the higher photocatalytic performance than rutile and brookite [34]. However, TiO_2 has a limited application under visible light irradiation because of its wide bandgap (3.2 eV for pure anatase TiO_2) [35]. The most common approach that proposed to expand the absorption edge of TiO_2 to the visible light region is by doping with transition metals (Fe, Mn, V) or non-metallic elements (N, C, S) [36–38]. Among these, nitrogen is the most favored anionic dopant due to its ability to modify the electronic structure of TiO_2 by leading the formation of new N 2p band above the O 2p valence band [39]. This modification decreases the bandgap of TiO_2 and eventually shifts the optical absorption of this semiconductor to the visible light region [40]. In addition, for the improvement of N-doped TiO_2 photocatalytic activity in the removal of heavy metals, the fabrication of porous structure is highly desirable due to its contribution increasing the specific surface area [41–43]. Following this path, it was reported that the porous structure of N-doped TiO_2 could afford more active sites for adsorption and photocatalytic reactions [44].

Various methods have been conducted to synthesize porous N-doped TiO_2, including the common-simple sol-gel method [45]. However, this method always involves a lot of organic solvents and organic titanium compound, which leads to harmful and corrosive chemical waste [46]. Therefore, the synthesis of porous N-doped TiO_2 by peroxo sol-gel method is believed to be an efficient and environmentally-friendly way to overcome this drawback as no organic solvent and organic titanium complex are involved [47,48]. Moreover, to the best of our knowledge, there is no report in the open literature that have been studied on environmentally-friendly preparation of N-doped TiO_2 supported by pore structure for photo-removal of Cd(II) ion. In this present work, we report the synthesis of porous N-doped TiO_2 by using PEG as an organic template through green peroxo sol-gel method for photocatalytic reduction of Cd(II) in the aqueous solutions under visible light irradiation. The optimum PEG concentration and the condition treatment effect on the photocatalytic reduction of Cd(II) by using this photocatalyst were investigated.

2. Materials and Methods

2.1 Materials

Titanium(IV) chloride ($TiCl_4$ 0.09 M in 20% HCl) and ammonium hydroxide (NH_4OH 25%) were purchased from Aldrich. Hydrogen peroxide (H_2O_2 30%) and polyethylene glycol 4000 (PEG 4000, $H(OCH_2CH_2)_nOH$), were purchased from Merck. All chemicals were used as received without any further purification.

2.2 Synthesis of Porous N-doped TiO_2

The synthesis method was adopted and modified moderately from our previous work [49]. Briefly, 36 mL $TiCl_4$ was slowly added into a 300 mL deionized water under vigorous magnetic stirring at temperature condition ~5 °C for 30 min. Then, the pH solution was adjusted to 10 by drop-wise addition of an aqueous ammonia solution and re-stirred for 24 h resulting in the formation of titanic acid white precipitates [$Ti(OH)_4$]. The obtained white precipitates were separated by centrifugation and repeatedly washed with deionized water to remove all of the Cl^- ions that formed in the reaction. After that the obtained precipitates were dispersed in 80 mL deionized water, followed by the addition of 28 mL H_2O_2 and different amount of PEG 4000 (0.7, 1.4 and 2.1 g) under constant stirring for 4 h at ambient

temperature, forming an aqueous transparent yellowish peroxotitanium complex (PTC). The product was vapored by using a rotary evaporator and dried at 105 °C. Finally, the obtained powders ware calcined on air at 500 °C for 1 h. The catalyst sample without PEG addition was labelled as NTO, others collected with 0.7, 1.4, and 2.1 g PEG were labelled as NTOP0.7, NTOP1.4, and NTOP2.1, respectively.

2.3 Catalysts Characterizations

The structural characterization of the catalysts was performed by X-ray diffraction (XRD, PANalytical CubiX^3) with Cu Kα radiation (λ = 1.5418 Å) at a scan rate of 8 (°)/min ranging from 20° to 80°. The optical property of the photocatalysts were observed by UV-Vis DRS, Shimadzu UV-Vis 2450 Spectrophotometer. Specific surface area (BET method) of the samples was measured using N_2 adsorption at 77 K in an automatic analyzer (Autosorb 6b, Quantachrome). The concentration of Cd(II)-alirazin red s complex was measured by UV-Vis spectrophotometry (Genesys 20).

2.4 Photocatalytic Activity Test

The photocatalytic reduction of Cd(II) on the porous N-doped TiO_2 was evaluated by using the batch technique. Here, 0.01 g of each the as-prepared photocatalyst was added to 100 mL of 5 mg/L Cd(II) aqueous solution at pH 5. The mixture was stirred for 30 min in the dark to reach adsorption/desorption equilibrium. Then, 10 mL of this sample was taken and irradiated under 24 W LED lamp in the photoreactor. The photocatalytic reduction was investigated at various reaction times of 0, 30, 60, 90, 120, and 150 min, respectively. Finally, the result mixture was centrifuged, and then the residual of Cd(II) in the filtrate was analyzed. The concentration of Cd(II) in aqueous solution was determined by the colorimetric method. In this method, 5 mL of the filtrate was added with alizarin red s as a coloring agent forming a complex solution. The absorption spectrum of this complex solution was measured by using UV-Vis spectrophotometer at λ = 422 nm.

3. Results and Discussion

3.1 Characterization of Porous N-doped TiO_2

Porous N-doped TiO_2 was synthesized through green peroxo sol-gel method using $TiCl_4$ and water as precursor and solvent, respectively. Here, the NH_4OH is contributed as a nitrogen source for N-doped TiO_2 photocatalyst. It has been reported that nitrogen would be incorporated into the TiO_2 lattice during the crystal transformation, leading to substitutional and/or interstitial doping [50] or adsorb on crystallite surface as NO_x species [48,51]. In order to form a porous structure, PEG was used as an organic templating agent. The pore formation was initiated by creating the PEG micelle through self-assembly [52]. Then, the weak coordination interaction between metallic Ti^{+4} and PEG micelle lead to the aggregation of Ti^{+4}-PEG globules composite [53]. After the thermal treatment, PEG would be decomposed into CO_2 and H_2O, forming a porous structure between particles.

The crystalline phase of the as-synthesized TiO_2 photocatalysts was determined by XRD. Figure 1(a–c) shows the typical XRD pattern of the NTO, NTOP0.7, and NTOP1.4 that can be assigned to the (101), (004), (200) and (211) crystal planes of anatase TiO_2 (ICCD, No. 01-084-1286). There are no peaks of brookite and rutile were detected, indicating high purity of these synthesized photocatalysts. On the other hand, the NTOP2.1 show different XRD pattern, which confirms the existence of both anatase and rutile crystalline phase. As can be seen in Figure 1(d), the distinctive peaks at 2θ = 27.4°, 36.1°, and 41.2° correspond to the (110), (101), and (111) crystal planes of rutile phase, respectively. Other peaks at 2θ = 54.3°, 62.7°, and 68.8° respectively correspond to the (211), (204), and (116) crystal planes of anatase phase. According to the Rietveld analysis, NTOP2.1 photocatalyst exhibited 90% of rutile and 10% of anatase crystalline phase, following the 01-071-0650 and 01-075-2553 files of ICCD

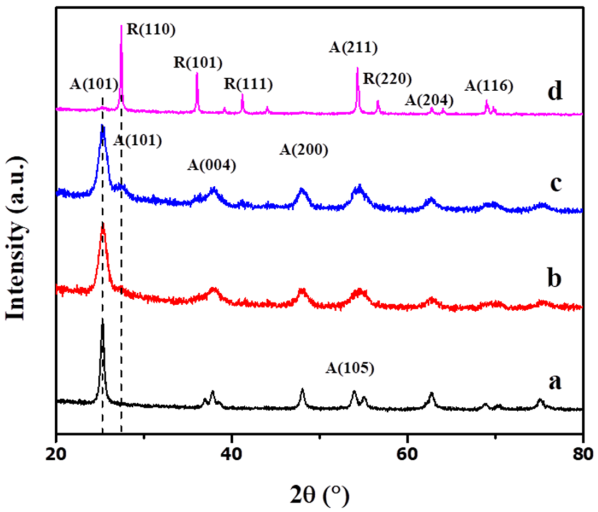

Figure 1. XRD pattern of (a) NTO, (b) NTOP0.7, (c) NTOP1.4, and (d) NTOP2.1.

database 2008. The obtained results revealed that the concentration of PEG addition affected the crystalline phase of synthesized N-doped TiO_2. Among the synthesized photocatalysts, the anatase phase was dominantly found in NTO and NTOP0.7. However, in NTOP1.4 which confirmed to be in the anatase phase, a small peak at $2\theta = 27.4^o$ is captured and further suggested as the initiation of rutile nucleation. Lončarević *et al.* [54] reported that rutile nucleation in the TiO_2 crystal structure is presumably caused by both of pore diameter and pore shrinkage, while the addition of PEG concentration beyond the optimal amount led to decrease in surface area due to the porous framework shrinkage during the thermal treatment. This phenomenon would produce TiO_2 with denser particles package and significantly reduce the porosity on the surface of this photocatalyst. The denser the particles network, the higher the orientation and frequency of anatase twin nucleation, which would lead to the rapid progression of anatase to rutile transformation. Therefore, it can be deduced that NTOP2.1 photocatalyst, the prepared sample with the highest amount of PEG, exhibited the

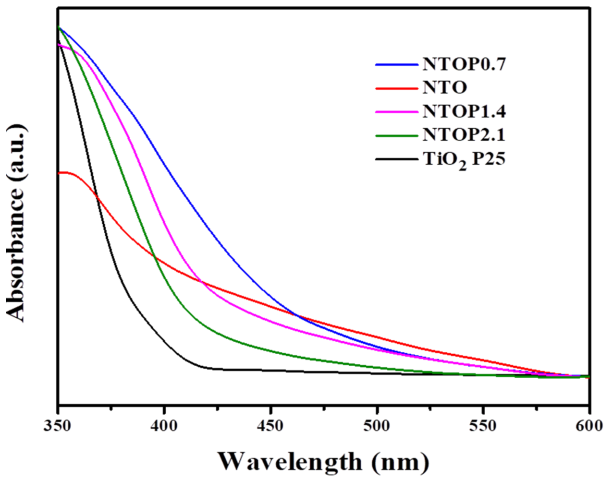

Figure 2. UV-Vis diffuse reflectance spectra of commercial TiO_2 (P25) and all N-doped TiO_2 samples.

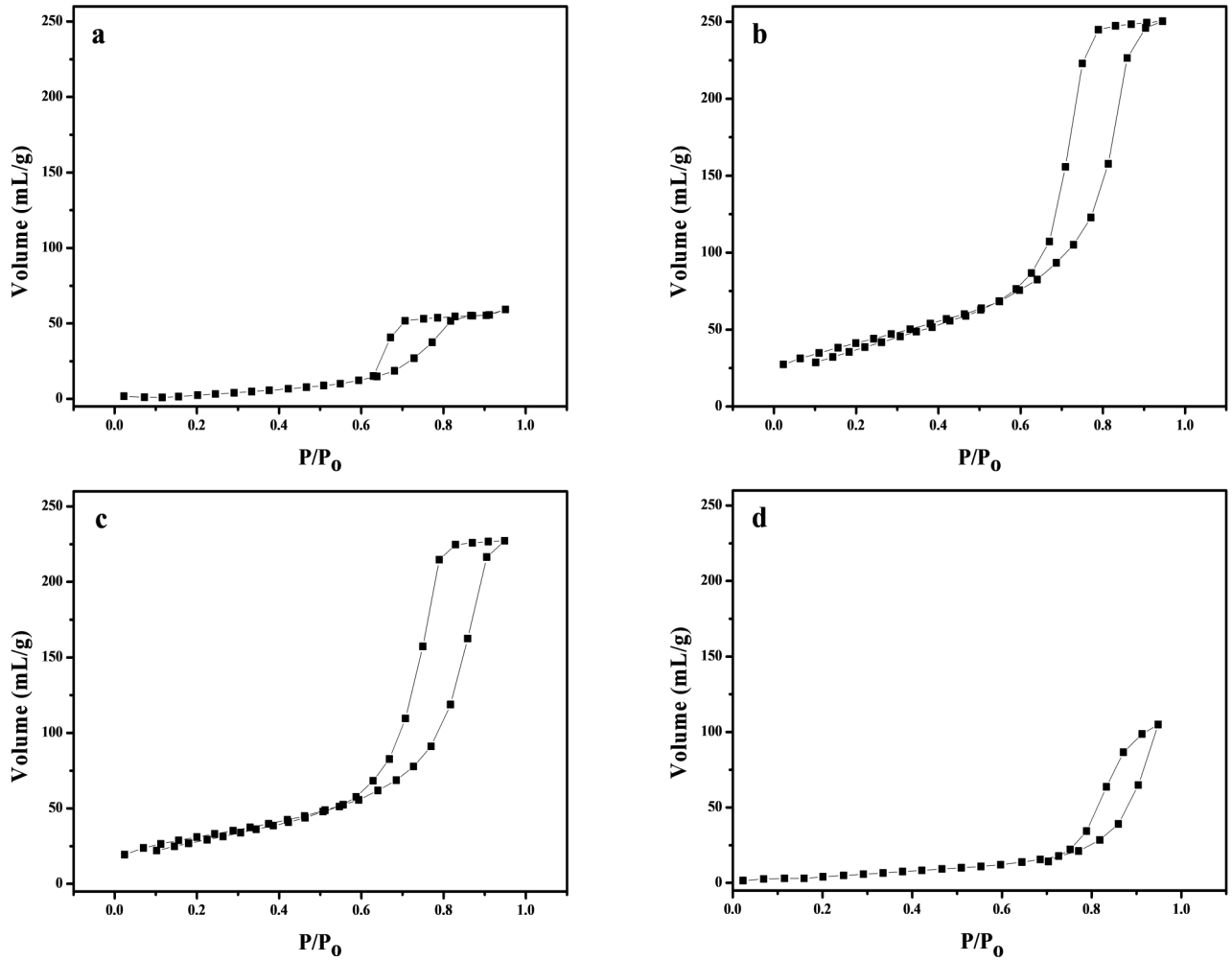

Figure 3. N_2 adsorption–desorption isotherm curves of (a) NTO, (b) NTOP0.7, (c) NTOP1.4, and (d) NTOP2.1.

highest rutile content as a consequence of the porous network damage [54].

The optical characterization of the synthesized photocatalyst was observed by UV-Vis DRS. As shown in Figure 2, all the TiO_2 photocatalysts that modified with nitrogen doping exhibit higher absorption in the visible light region than that of the commercial TiO_2 (P25). By applying the Tauc plot and Kubelka-Munk function, the band gap energies were calculated as 3.28 eV; 2.85 eV; 2.96 eV; 2.91 eV; and 2.90 eV for the commercial TiO_2 (P25) Degussa, NTO, NTOP0.7, NTOP1.4, and NTOP2.1, respectively. It is confirmed that the contribution of nitrogen doping narrowed the bandgap energy of the synthesized photocatalysts by leading the formation of new N 2p band between the O 2p and Ti 3d valence band in the TiO_2 electronic structure [55]. With the corresponding of the lower bandgap energy, the synthesized photocatalyst can trigger the electron migration from the valence band to the conduction band by absorbing energy from the visible light region [40].

The isotherms of N_2 adsorption-desorption were recorded to evaluate the porous properties of all the synthesized photocatalysts. As shown in Figure 3(a–d), the typical type IV-isotherm curve was observed, indicating the characteristic of mesoporous material with average pore distribution in the range of 3–6 nm. The BET surface area, the total pore volume as well as the pore diameter for all the synthesized photocatalysts were detailed in Table 1. In this study, it showed that the addition of PEG as an organic template caused the increase of porous structure of the unmodified sample. All NTOP samples had higher BET surface area, diameter of pore and volume of pore than the sample without PEG addition. Among modified samples, the largest BET surface area was NTOP0.7 sample. However, a decrease in the specific surface area was observed as the PEG addition increased [54]. This obtained results confirmed that the addition of PEG over the optimal amount leads to the porous network shrinkage.

3.2 Photocatalytic Activity of the Photocatalyst

The adsorption and the photocatalytic reduction of Cd(II) using all the as-synthesized porous N-doped TiO_2 ware evaluated by examining the percentage removal of Cd(II) under dark and light condition [56]. Here, NTOP0.7; NTOP1.4; and NTOP2.1 photocatalyst were used for photocatalytic reduction of Cd(II) under visible light irradiation and compared with the NTO photocatalyst (Figure 4). Figure 4(a)

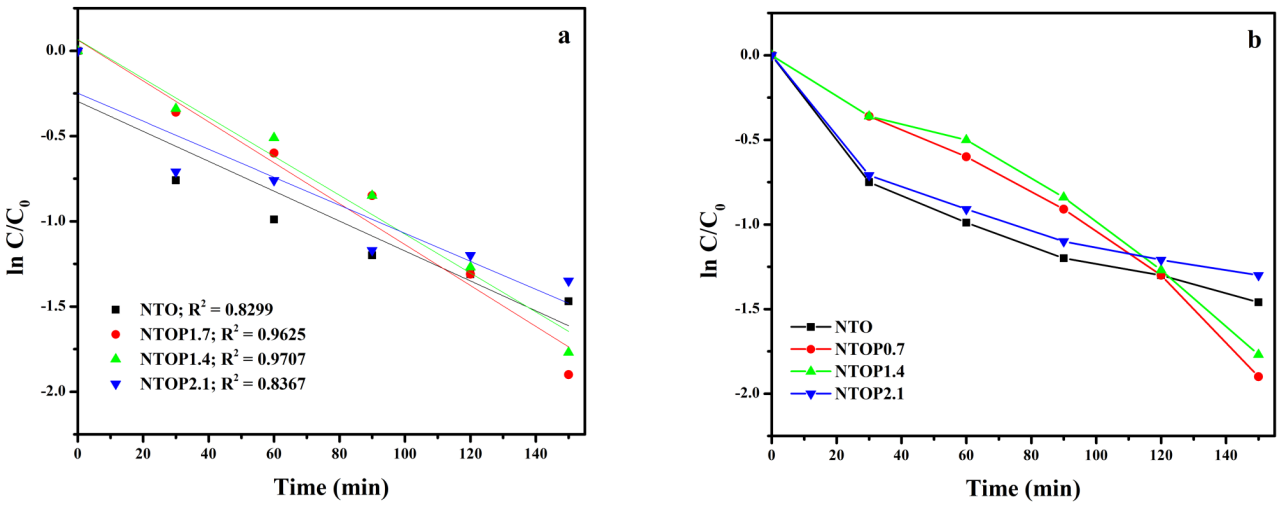

Figure 4. Photocatalytic reduction of Cd(II) using all the prepared TiO_2 samples (a) with and (b) without irradiation. Applied condition: catalyst mass: 0.01 g, solution volume: 100 mL and initial concentration of Cd(II): 5 mg/L, pH 5, 24 W-LED visible light.

Table 1. Specific surface area, diameter and volume of all as-prepared photocatalysts.

No	Sample	Specific surface area (m^2/g)	Diameter of pore (nm)	Volume of pore (mL/g)
1	NTO	50.4	3.6	0.1
2	NTOP0.7	236.9	3.9	0.4
3	NTOP1.4	204.1	3.9	0.4
4	NTOP2.1	72.5	5.6	0.2

showed that with 5 mg/L of Cd(II), NTOP0.7 exhibited the highest reduction efficiency than NTOP0.4; NTOP2.1 and NTO photocatalyst after 150 min of visible light irradiation. At the same condition, the adsorption control experiments were carried out to study the adsorption ability of NTOP0.7; NTOP1.4; and NTOP2.1 toward Cd(II) under dark condition (Figure 4(b)). The result shows that NTOP0.7 has the highest adsorption efficiency among the other photocatalyst sample due to the high specific surface area according to BET analysis. It is described

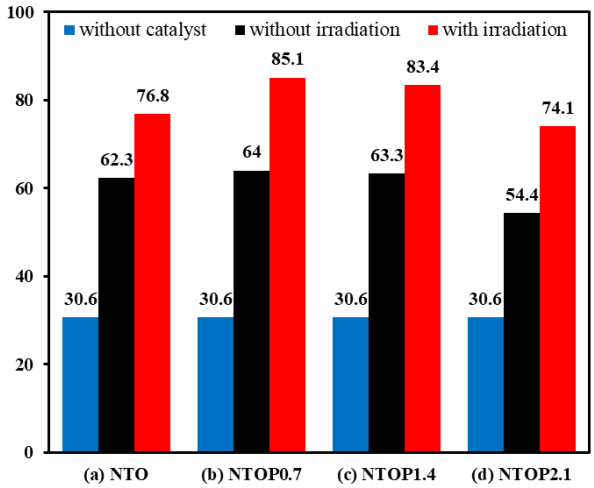

Figure 5. The percentage of Cd(II) removal chart using (a) NTO (b) NTOP0.7 (c)NTOP1.4 and (d) NTOP2.1 under visible light irradiation for 150 min.

that the photocatalytic reduction of Cd(II) pattern followed the pseudo first-order kinetic model. The kinetic rate equation is expressed in Equation (1).

$$\ln\left(\frac{C}{C_0}\right) = -K_{app}t \quad (1)$$

where, C_0 is the initial Cd(II) concentration, C is the Cd(II) concentration at reaction time t, and K_{app} is the pseudo first order rate constant. Values of the pseudo first-order parameters for all as-synthesized samples was determined in Table 2. The order photocatalytic activity was found to be: NTOP0.7 > NTOP1.4 > NTO > NTOP2.1. As shown in Figure 5, it was found that the highest percentage of Cd(II) removal was successfully accomplished by NTOP0.7 under visible light irradiation for 150 min at pH 5. Approximately 85.1% of Cd(II) was removed from the aqueous solutions in the presence of this photocatalyst via photocatalytic reduction. Meanwhile, only 83.4%, 76.8%, and 74.1% of Cd(II) were removed by NTOP1.4, NTO, and NTOP2.1, respectively. Lončarević *et al.* [54] reported that BET surface area and anatase fraction, were found to be the most important factors governing the photocatalytic activity. Therefore, the obtained results indicated that modified N-doped TiO_2 photocatalyst with the specified amount of PEG exhibited higher activity than other photocatalyst samples due to higher specific surface area and higher fraction of active anatase phase.

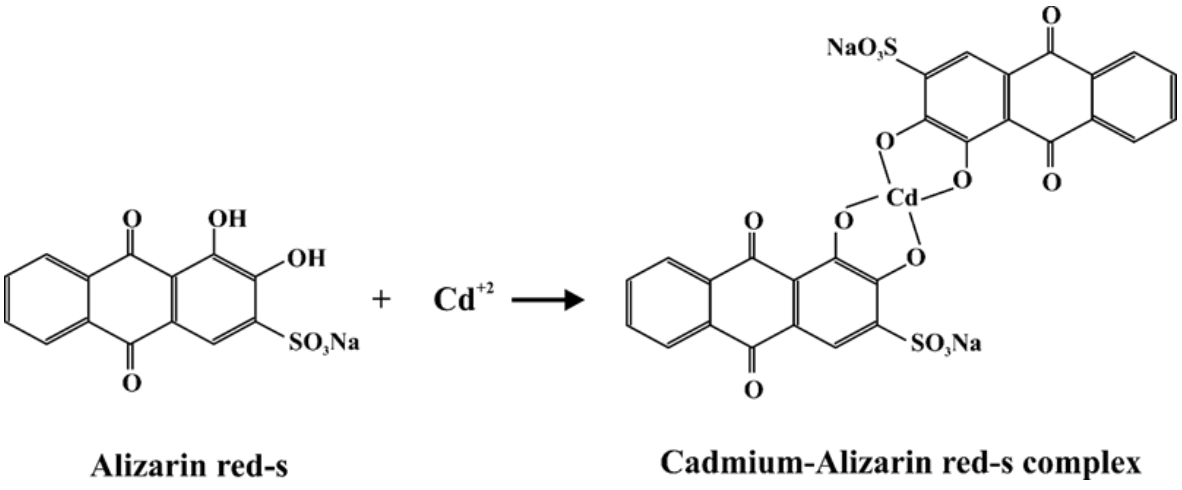

Figure 6. Complex reaction of alizarin red-s with Cd(II).

Table 2. Pseudo-first order parameters for Cd (II) photoreduction.

No	Sample	K_{app} (min^{-1})	R^2 values
1	NTO	0.009	0.86
2	NTOP0.7	0.012	0.97
3	NTOP1.4	0.011	0.98
4	NTOP2.1	0.008	0.87

The photocatalytic reduction mechanism of Cd(II) by using porous N-doped TiO_2 under visible light irradiation is given by the following net reactions [24,25,28,52]:

Excitation:

$$TiO_2 + hv \text{ (visible light)} \rightarrow e^- + h^+ \quad (2)$$

Photocatalytic reduction:

$$Cd^{2+} + 2e^- \rightarrow Cd^0 \quad (3)$$

The trace amount of toxic Cd(II) after the photocatalytic reduction was determined by spectrophotometer method using the alizarin red-s as a spectrophotometric reagent. Figure 6 shows the reaction between Cd(II) ion and alizarin red-s dye. The cadmium-alizarin red-s complex gives a specific color of deep greenish-yellow [57]. Figure 7 shows the absorbance of the cadmium-alizarin red-s complex solution before and after photocatalytic treatment by NTOP0.7 photocatalyst under visible light irradiation. The maximum peak of this complex solution was measured at 422 nm. It was found that the absorbance peak of cadmium-alizarin red-s complex solution significantly decreased after the photocatalytic treatment, indicating the excellent photocatalytic activity of NTOP0.7 in reducing the toxic Cd(II) ion.

4. Conclusions

Porous N-doped TiO_2 photocatalyst has been successfully synthesized by green peroxo sol gel method using polyethylene glycol (PEG) as an organic templating agent. The optimal PEG addition for the synthesis of porous N-doped TiO_2 with high surface area and excellent photocatalytic activity was 0.7 g. The highest photocatalytic reduction of Cd(II) was about 85.1% by using NTOP0.7 photocatalyst under visible light irradiation for 150 min, while the percentage adsorption of Cd(II) without irradiation was 64%, and the percentage removal of Cd(II) without photocatalyst in the acid condition was 30.65%. It was clearly found that porous N-doped TiO_2 performed a highly photocatalytic active site that can afford for the adsorption and photocatalytic reactions of Cd(II) removal in aqueous solution.

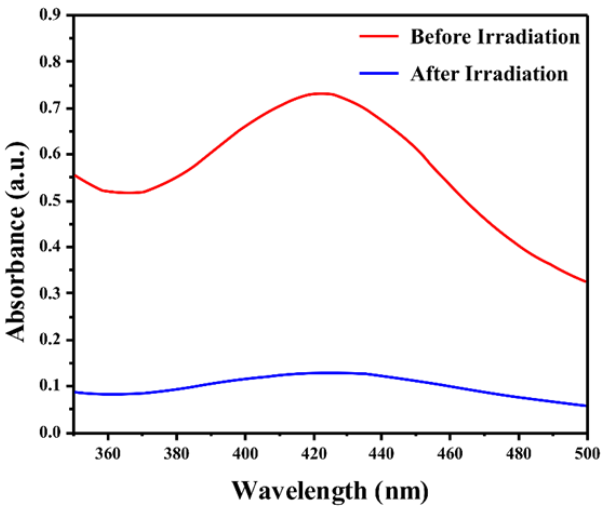

Figure 7. UV-Vis spectrum of cadmium-alizarin red-s complex before and after photocatalytic treatment using NTOP0.7 photocatalyst under visible light irradiation.

Acknowledgements

Authors gratefully acknowledge the financial support from Indonesian Ministry of Research, Technology and Higher Education through Student Creativity Program-2019.

References

[1] Khairy, M., El-Safty, S.A., Shenashen, M.A. (2014). Environmental remediation and monitoring of cadmium. *TrAC - Trends in Analytical Chemistry*, 62, 56–68. DOI: 10.1016/j.trac.2014.06.013.

[2] Sharma, H., Rawal, N., Mathew, B.B. (2015). The Characteristics, Toxicity and Effects of Cadmium. *International Journal of Nanotechnology and Nanoscience*, 3, 1–9.

[3] Kinuthia, G.K., Ngure, V., Beti, D., Lugalia, R., Wangila, A., Kamau, L. (2020). Levels of heavy metals in wastewater and soil samples from open drainage channels in Nairobi, Kenya: community health implication. *Scientific Reports*, 10, 1–13. DOI: 10.1038/s41598-020-65359-5.

[4] Naeemullah. N., Kazi, T.G., Afridi, H.I., Shah, F., Arain, S.S., Brahman, K.D., Ali, J., Arain, M.S. (2016). Simultaneous determination of silver and other heavy metals in aquatic environment receiving wastewater from industrial area, applying an enrichment method. *Arabian Journal of Chemistry*, 9, 105–113. DOI: 10.1016/j.arabjc.2014.10.027.

[5] Ravera, O. (1986). *Cadmium in freshwater ecosystems*. In: Mislin H, Ravera O (eds) Cadmium in the Environment. Birkhäuser Basel, Basel, pp 75–87.

[6] Kubier, A., Wilkin, R.T., Pichler, T. (2019). Cadmium in soils and groundwater: A review. *Applied Geochemistry*, 108, 104388. DOI: 10.1016/j.apgeochem.2019.104388.

[7] Rahimzadeh, M.R., Rahimzadeh, M.R., Kazemi, S., Moghadamnia, A.A. (2017). Cadmium toxicity and treatment: An update. *Caspian Journal of Internal Medicine*, 8, 135–145. DOI: 10.22088/cjim.8.3.135.

[8] Genchi, G., Sinicropi, M.S., Lauria, G., Carocci, A., Catalano, A. (2020). The Effects of Cadmium Toxicity. *International Journal of Environmental Research and Public Health*, 17, 3782. DOI: 10.3390/ijerph17113782.

[9] Zhang, H., Reynolds, M. (2019). Cadmium exposure in living organisms: A short review. *Science of the Total Environment*, 678, 761–767. DOI: 10.1016/j.scitotenv.2019.04.395.

[10] Aoshima, K. (2019). *Recent Clinical and Epidemiological Studies of Itai-Itai Disease (Cadmium-Induced Renal Tubular Osteomalacia) and Cadmium Nephropathy in the Jinzu River Basin in Toyama Prefecture, Japan*. In: Cadmium Toxicity. Springer, Singapore, pp 23–37.

[11] Morikawa, Y., Nakagawa, H., Tabata, M., Nishijo, M., Senma, M., Kitagawa, Y., Kawano, S., Teranishi, H., Kido, T. (1992). Study of an outbreak of Itai-itai disease. *Japanese Journal of Hygiene*, 46, 1057–1062. DOI: 10.1265/jjh.46.1057.

[12] Wong, C.W., Barford, J.P., Chen, G., McKay, G. (2014). Kinetics and equilibrium studies for the removal of cadmium ions by ion exchange resin. *Journal of Environmental Chemical Engineering*, 2, 698–707. DOI: 10.1016/j.jece.2013.11.010.

[13] Bayar, S., Yilmaz, A.E., Boncukcuoğlu, R., Fil, B.A., Kocakerim, M.M. (2013). Effects of operational parameters on cadmium removal from aqueous solutions by electrochemical coagulation. *Desalination and Water Treatment*, 51, 2635–2643. DOI: 10.1080/19443994.2012.749201.

[14] Esalah, J.O., Weber, M.E., Vera, J.H. (2000). Removal of lead, cadmium and zinc from aqueous solutions by precipitation with sodium di-(n-octyl) phosphinate. *Canadian Journal of Chemical Engineering*, 78, 948–954. DOI: 10.1002/cjce.5450780512.

[15] Karim, M.R., Aijaz, M.O., Alharth, N.H., Alharbi, H.F., Al-Mubaddel, F.S., Awual, M.R. (2019). Composite nanofibers membranes of poly(vinyl alcohol)/chitosan for selective lead(II) and cadmium(II) ions removal from wastewater. *Ecotoxicology and Environmental Safety*, 169, 479–486. DOI: 10.1016/j.ecoenv.2018.11.049.

[16] Tabesh, S., Davar, F., Loghman-Estarki, M.R. (2018). Preparation of γ-Al2O3 nanoparticles using modified sol-gel method and its use for the adsorption of lead and cadmium ions. *Journal of Alloys and Compounds*, 730, 441–449. DOI: 10.1016/j.jallcom.2017.09.246.

[17] Rao, K., Mohapatra, M., Anand, S., Venkateswarlu, P. (2011). Review on cadmium removal from aqueous solutions. *International Journal of Engineering, Science and Technology*, 2, 81–103. DOI: 10.4314/ijest.v2i7.63747.

[18] Chen, D., Ray, A.K. (2001). Removal of toxic metal ions from wastewater by semiconductor photocatalysis. *Chemical Engineering Science*, 56, 1561–1570. DOI: https://doi.org/10.1016/S0009-2509(00)00383-3.

[19] Shaikh, A., Mishra, S.P., Mohapatra, P., Parida, S. (2017). One-step solvothermal synthesis of TiO2-reduced graphene oxide nanocomposites with enhanced visible light photoreduction of Cr(VI). *Journal of Nanoparticle Research*, 19, 1-9. DOI: 10.1007/s11051-017-3894-7.

[20] Le, A.T., Pung, S.-Y., Sreekantan, S., Matsuda, A., Huynh, D.P. (2019). Mechanisms of removal of heavy metal ions by ZnO particles. *Heliyon*, 5, e01440. DOI: 10.1016/j.heliyon.2019.e01440.

[21] Nasr, M., Eid, C., Habchi, R., Miele, P., Bechelany, M. (2018). Recent Progress on Titanium Dioxide Nanomaterials for Photocatalytic Applications. *ChemSusChem*, 11, 3023–3047. DOI: 10.1002/cssc.201800874.

[22] Hosseini, F., Mohebbi, S. (2020). High efficient photocatalytic reduction of aqueous Zn2+, Pb2+ and Cu2+ ions using modified titanium dioxide nanoparticles with amino acids. *Journal of Industrial and Engineering Chemistry*, 85, 190–195. DOI: 10.1016/j.jiec.2020.01.040.

[23] Liu, F., Zhang, W., Tao, L., Hao, B., Zhang, J. (2019). Simultaneous photocatalytic redox removal of chromium(VI) and arsenic(III) by hydrothermal carbon-sphere@nano-Fe3O4. *Environmental Science: Nano*, 6, 937–947. DOI: 10.1039/c8en01362d.

[24] Salmanvandi, H., Rezaei, P., Tamsilian, Y. (2020). Photoreduction and Removal of Cadmium Ions over Bentonite Clay-Supported Zinc Oxide Microcubes in an Aqueous Solution. *ACS Omega*, 5, 13176–13184. DOI: 10.1021/acsomega.0c01219.

[25] Ekwere, I.O., Horsfall, M., Otaigbe, J.O.E. (2019). A Study on the Photocatalytic Reduction of Some Metal Ions in Aqueous Solution Using UV- Titanium Dioxide System. *International Research Journal of Pure and Applied Chemistry*, 18, 1–7. DOI: 10.9734/irjpac/2019/v18i230087.

[26] Stroyuk, A.L., Shvalagin, V.V., Raevskaya, A.E., Korzhak, A.V., Kuchmii, S.Y. (2003). Photocatalysis of the reduction of Cd^{2+} ions by Cds nanoparticles in isopropyl alcohol. *Theoretical and Experimental Chemistry*, 39, 341–346. DOI: 10.1023/B:THEC.0000013985.94005.c3.

[27] Chowdhury, P., Elkamel, A., Ray, A.K. (2015). *Photocatalytic Processes for the Removal of Toxic Metal Ions*. In: Heavy Metals In Water. Royal Society of Chemistry, Cambridge, pp 25–43.

[28] Chowdhury, P., Athapaththu, S., Elkamel, A., Ray, A.K. (2017). Visible-solar-light-driven photo-reduction and removal of cadmium ion with Eosin Y-sensitized TiO_2 in aqueous solution of triethanolamine. *Separation and Purification Technology*, 174, 109–115. DOI: 10.1016/j.seppur.2016.10.011.

[29] Gopinath, K.P., Madhav, N.V., Krishnan, A., Malolan, R., Rangarajan, G. (2020). Present applications of titanium dioxide for the photocatalytic removal of pollutants from water: A review. *Journal of Environmental Management*, 270, 110906. DOI: 10.1016/j.jenvman.2020.110906.

[30] Cai, J., Wu, X., Zheng, F., Li, S., Wu, Y., Lin, Y., Lin, L., Liu, B., Chen, Q., Lin, L. (2017). Influence of TiO_2 hollow sphere size on its photo-reduction activity for toxic Cr(VI) removal. *Journal of Colloid and Interface Science*, 490, 37–45. DOI: 10.1016/j.jcis.2016.11.025.

[31] Sane, P., Chaudhari, S., Nemade, P., Sontakke, S. (2018). Photocatalytic reduction of chromium(VI) using combustion synthesized TiO2. *Journal of Environmental Chemical Engineering*, 6, 68–73. DOI: 10.1016/j.jece.2017.11.060.

[32] Wellia, D.V., Wulandari, W., Mustaqimah, A., Pratiwi, N., Putri, Y.E. (2020). Fabrication of Superhydrophobic Film on the Surface of Indonesian Bamboo Timber by TiO_2 Deposition and Using Octadecyltrichlorosilane as a Surface Modifier Agent. *Indonesian Journal of Chemistry*, 20, 870. DOI: 10.22146/ijc.46740.

[33] Pratiwi, N., Zulhadjri, Z., Arief, S., Wellia, D.V. (2020). A Facile Preparation of Transparent Ultrahydrophobic Glass via TiO_2/Octadecyltrichlorosilane (ODTS) Coatings for Self-Cleaning Material. *ChemistrySelect*, 5, 1450–1454. DOI: 10.1002/slct.201904153.

[34] Zhang, J., Zhou, P., Liu, J., Yu, J. (2014). New understanding of the difference of photocatalytic activity among anatase, rutile and brookite TiO_2. *Physical Chemistry Chemical Physics*, 16, 20382–20386. DOI: 10.1039/c4cp02201g.

[35] Thind, S.S., Wu, G., Chen, A. (2012). Synthesis of mesoporous nitrogen–tungsten co-doped TiO_2 photocatalysts with high visible light activity. *Applied Catalysis B, Environmental"*, 111–112, 38–45. DOI: 10.1016/j.apcatb.2011.09.016.

[36] Reddy, K.M., Baruwati, B., Jayalakshmi, M., Rao, M.M., Manorama, S.V. (2005). S-, N- and C-doped titanium dioxide nanoparticles: Synthesis, characterization and redox charge transfer study. *Journal of Solid State Chemistry*, 178, 3352–3358. DOI: 10.1016/j.jssc.2005.08.016.

[37] Dua, J., Chen, H., Yang, H., Sang, R., Qian, Y., Li, Y., Zhu, G., Mau, Y., He, W., Joon, D. (2013). A facile sol – gel method for synthesis of porous Nd-doped TiO_2 monolith with enhanced photocatalytic activity under UV – Vis irradiation. *Microporous and Mesoporous Materials*, 182, 87–94. DOI: 10.1016/j.micromeso.2013.08.023.

[38] Liu, Z., Ya, J., Lei, E., Xin, Y., Zhao, W. (2010). Effect of V doping on the band-gap reduction of porous TiO_2 films prepared by sol-gel route. *Materials Chemistry and Physics*, 120, 277–281. DOI: 10.1016/j.matchemphys.2009.11.008.

[39] Chen, Y., Liu, K. (2016). Preparation of granulated N-doped TiO_2/diatomite composite and its applications of visible light degradation and disinfection. *Powder Technology*, 303, 176–191. DOI: 10.1016/j.powtec.2016.09.038.

[40] Ansari, S.A., Khan, M.M., Ansari, M.O., Cho, M.H. (2016). Nitrogen-doped titanium dioxide (N-doped TiO_2) for visible light photocatalysis. *New Journal of Chemistry*, 40, 3000–3009. DOI: 10.1039/C5NJ03478G.

[41] Li, X., Liu, P., Mau, Y., Xing, M., Zhang, J. (2015). Preparation of homogeneous nitrogen-doped mesoporous TiO2 spheres with enhanced visible-light photocatalysis. *Applied Catalysis B: Environmental*, 164, 352–359. DOI: 10.1016/j.apcatb.2014.09.053.

[42] Xia, L., Yang, Y., Cao, Y., Liu, B., Li, X., Chen, X., Song, H., Zhang, X., Gao, B., Fu, J. (2019). Porous N-doped TiO_2 nanotubes arrays by reverse oxidation of TiN and their visible-light photocatalytic activity. *Surface and Coatings Technology*, 365, 237–241. DOI: 10.1016/j.surfcoat.2018.06.033.

[43] Wellia, D.V., Kusumawati, Y., Diguna, L.J., Pratiwi, N., Putri, R.A., Amal, M.I. (2020). *Mesoporous Materials for Degradation of Textile Dyes*. In: Green Methods for Wastewater Treatment. pp 255–288.

[44] Horikawa, T., Katoh, M., Tomida, T. (2008). Preparation and characterization of nitrogen-doped mesoporous titania with high specific surface area. *Microporous and Mesoporous Materials*, 110, 397–404. DOI: 10.1016/j.micromeso.2007.06.048.

[45] Zhao, W., Liu, S., Zhang, S., Wang, R., Wang, K. (2019). Preparation and visible-light photocatalytic activity of N-doped TiO_2 by plasma-assisted sol-gel method. *Catalysis Today*, 337, 37–43. DOI: 10.1016/j.cattod.2019.04.024.

[46] Danks, A.E., Hall, S.R., Schnepp, Z. (2016). The evolution of "sol-gel" chemistry as a technique for materials synthesis. *Materials Horizons*, 3, 91–112. DOI: 10.1039/c5mh00260e.

[47] Wellia, D.V., Fitria, D., Safni, S. (2018). C-N-Codoped TiO_2 Synthesis by using Peroxo Sol Gel Method for Photocatalytic Reduction of Cr(VI). *The Journal of Pure and Applied Chemistry Research*, 7, 26–32. DOI: 10.21776/ub.jpacr.2018.007.01.373.

[48] Xu, Q.C., Wellia, D. V., Amal, R., Liao, D.W., Loo, S.C.J., Tan, T.T.Y. (2010). Superhydrophilicity-assisted preparation of transparent and visible light activated N-doped titania film. *Nanoscale*, 2, 1122–1127. DOI: 10.1039/c005273f.

[49] Pratiwi, N., Zulhadjri, Z., Arief, S., Admi, A., Wellia, D.V. (2020). Self-cleaning material based on superhydrophobic coatings through an environmentally friendly sol–gel method. *Journal of Sol-Gel Science and Technology*, 96, 669–678. DOI: 10.1007/s10971-020-05389-7.

[50] Qiu, X., Zhao, Y., Burda, C. (2007). Synthesis and characterization of nitrogen-doped group IVB visible-light-photoactive metal oxide nanoparticles. *Advanced Materials*, 19, 3995–3999. DOI: 10.1002/adma.200700511.

[51] Xu, Q.C., Wellia, D.V., Yan, S., Liao, D.W., Lim, T.M., Tan, T.T.Y. (2011). Enhanced photocatalytic activity of C-N-codoped TiO_2 films prepared via an organic-free approach. *Journal of Hazardous Materials*, 188, 172–180. DOI: 10.1016/j.jhazmat.2011.01.088.

[52] Butun, S., Demirci, S., Yasar, A.O., Sagbas, S., Aktas, N., Sahiner, N. (2017). *0D, 1D, 2D, and 3D Soft and Hard Templates for Catalysis*, 1st ed. In: Studies in Surface Science and Catalysis, 1st ed. Elsevier B.V., pp 317–357.

[53] Tu, L., Pan, H., Xie, H., Yu, A., Xu, M., Chai, Q., Cui, Y., Zhou, X. (2012). Study on the fabrication and photovoltaic property of TiO_2 mesoporous microspheres. *Solid State Sciences*, 14, 616–621. DOI: 10.1016/j.solidstatesciences.2012.02.012.

[54] Lončarević, D., Dostanić, J., Radonjić, V., Radosavljević-Mihajlović, A., Jovanović, D.M. (2015). Structure-activity relationship of nanosized porous PEG-modified TiO2 powders in degradation of organic pollutants. *Advanced Powder Technology*, 26, 1162–1170. DOI: 10.1016/j.apt.2015.05.012.

[55] Huang, L., Fu, W., Fu, X., Zong, B., Liu, H., Bala, H., Wang, X., Sun, G., Cao, J., Zhang, Z. (2017). Facile and large-scale preparation of N doped TiO2 photocatalyst with high visible light photocatalytic activity. *Materials Letters*, 209, 585–588. DOI: 10.1016/j.matlet.2017.08.092.

[56] Chen, F., Yu, W., Qie, Y., Zhao, L., Zhang, H., Guo, L.H. (2019). Enhanced photocatalytic removal of hexavalent chromium through localized electrons in polydopamine-modified TiO2 under visible irradiation. *Chemical Engineering Journal*, 373, 58–67. DOI: 10.1016/j.cej.2019.05.022.

[57] Ullah, M., Haque, M.E. (2010). Spectrophotometric Determination of Toxic Elements (Cadmium) in Aqueous Media. *Journal of Chemical Engineering*, ChE. 25, 1–12. DOI: 10.3329/jce.v25i0.7233.